Soft Computing (2019) 23:8839–8853
https://doi.org/10.1007/s00500-018-3483-4

METHODOLOGIES AND APPLICATION

A particle swarm optimization, fuzzy PID controller with generator automatic voltage regulator

Abdullah J. H. Al Gizi[1]

Published online: 31 August 2018

Abstract

The role of an intelligent control system with a certain stage of autonomy is prerequisite for effective operation. We designed a particle swarm optimization, fuzzy proportional integral derivative (PSOFPID) controller using MATLAB for a set point voltage and frequency. The projected controller intended to ease the frequency and the terminal potential difference constantly under any operating conditions and loads which can be attained in the wanted range via the rule of the generation system. PSOFPID used to carry out the AVR system auctions main voltage control. The existing algorithm was based on particle swarm optimization (PSO), and Sugeno fuzzy logic (SFL). It required optimal tuning for thematic factory operation of the generation system. The newly developed controller combined the PSO and fuzzy logic control (FLC) to determine the optimal PID controller of generator parameters in the AVR system. The PSOFPID controller was used as a hybrid full control system for the voltage and frequency. Optimal PID gains obtained by a combined PSO and SFL for various operating conditions of PSO (β and know about birds' no.) were employed to develop the principle subject of the Sugeno fuzzy system. The hybrid controller arranged the control signal based on communication and thereby decreases the voltage error and the swaying in the terminal voltage and frequency control process. An outstanding potential and frequency control presentation was achieved when the projected hybrid controller was broken on the AVR system in synchronous generator to improve the transient response.

Graphical abstract

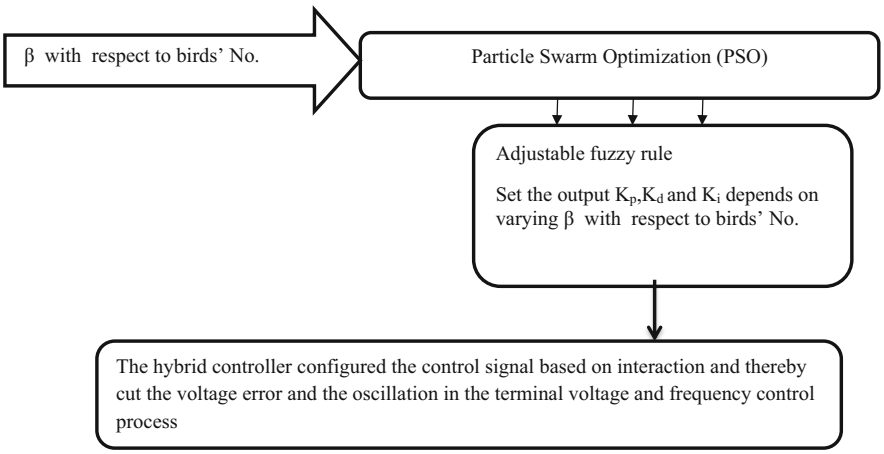

Keywords AVR · PSOFPID · PSO · SFL · FLC

Communicated by V. Loia.

✉ Abdullah J. H. Al Gizi
abdullh969@yahoo.com

[1] Southern Technical University, Al Basrah, Iraq

1 Introduction

The AVR is employed for checking the terminal voltage by adapting the voltage of the generator, while the AVR system optimal control is accomplished by the PID inside the AVR. Thus, the design of an effective and efficient fractional-order PID (FOPID) controller as a generalization of a standard PID controller based on fractional-order (FO) calculus is required (Zeng et al. 2015). An FO PID (FOPID) controller is designed for an automatic voltage regulator (AVR) system with broader performance objectives (Pan and Das 2013). Furthermore, FOPID controller is an application of fractional calculus theory in PID controller (Chen et al. 2014). FOPID controllers are designed for load–frequency control (LFC) of two interconnected power systems (Pan and Das 2015). A stochastic multi-parameters divergence method for online parameter optimization of fractional-order proportional–integral–derivative (PID) controllers was presented (Yeroğlu and Ateş 2014). An adaptive optimal control design approach was followed for automatic voltage regulator (AVR) system where policy iteration technique based adaptive critic scheme was utilized (Prasad et al. 2014). An application and analysis of an integer order (IO) as well as fractional order (FO). A system was proposed based on proportional integral derivative (PID) controller for speed regulation in a chopper fed direct current (DC) motor drive (Rajasekhar et al. 2014). A chaotic ant swarm optimization (CASO) was utilized to tune the parameters of both single-input and dual-input power system stabilizers (PSSs) (Chatterjee et al. 2011). The additional parameters of differ-integral orders on the one hand rendered more flexibility to the fractional-order elements which were essentially infinite dimensional filters (Pan and Das 2012b). The optimum PID limits required to formulate the fuzzy rule table were generated via the real-coded genetic algorithm (RGA) (Devaraj and Selvabala 2009). The RBF-NN produced the robust response near the midpoint of the Gaussian Kernel function, where each hidden node in the input data space was soon as a local detector (Qasem and Shamsuddin 2011; Al-geelani et al. 2012). Furthermore, the RBF-NN was deliberate as a local estimation model of the controlled process without requiring a special distribution. RBF being an online learning could converge rapidly. Consequently, the control field for implementing the real-time manipulation focused on the NN.

Earlier, RBF was applied to obtain the best controller parameters to keep the system error zero (Yao-Lun et al. 2007). Based on distributed intelligence rather than traditional centralized control, a new approach to power system automation was introduced (Simoes et al. 1997). Using the optimal robust control methodology, a hydraulic turbine generator governor was designed and analyzed (Jiang 1995). A comprehensive review on advanced control techniques for micro-grids (Guerrero et al. 2013) covered the decentralized, distributed, and hierarchical control of grid connected and islanded to micro-grids. Another novel approach to power system automation was suggested (Higgins et al. 2011). An intelligent fuzzy logic controller was proposed to control effectively the frequency and voltage of a power generating system (Soundarrajan and Sumathi 2010). In this controller, the load frequency control (LFC) and automatic voltage regulator (AVR) was installed in each generator to regulate the real and reactive power flows. A best PID controller for a universal second-order system was improved using a linear-quadratic regulator (LQR) method (Yu and Hwang 2004). This approach required an appropriate weighting function for acceptable performance.

Minglin (2010) proposed a method for designing PID-like fuzzy controller with FPGAv. The feed forward fuzzy PID (FFFPID) controller was used to improve the performance of high pressure common rail system (Su et al. 2010). Sinthipsomboon et al. (Chatterjee et al. 2011; Prasad et al. 2014; Rajasekhar et al. 2014; Yeroğlu and Ateş 2014) used computational methods such as GA and fuzzy for methodical answer of FFFPID controller. A joint fuzzy and fuzzy self-tuning PID controller was projected to overcome the limits of the current mix fuzzy PID controller presentation, where system parameters alterations required a new PID controller adjustment variable (Sinthipsomboon et al. 2011). An enhanced Fuzzy PID controller was used (Arulmozhiyal 2012; Arulmozhiyal and Kandiban 2012) to control the rapidity of brushless DC motor. PLC was used to develop a fuzzy PID controller for a set point pressure control in the main pressure collection system (Chen et al. 2012). The design and stability analysis of Takagi–Sugeno–Kang (TSK)-type full-scale fuzzy proportional integral derivative (PID) controller was achieved (Jinwook et al. 2012). Boundary self-setting fuzzy PID control process was applied to control drying temperature for refining the temperature variations (Man-chen and Ling-long 2012). An better fuzzy PID controller procedure was planned based on DSP (Zhang Xiao and Long Shi 2012).

In contrast to NSGA-II-based FOPID project procedure, the projected MOEO procedure accepted individual-based repeated optimization mechanism with only polynomial mutation named mutation operation. From the viewpoint of procedure design, the projected MOEO procedure was relatively simpler than NSGA-II (Pan and Das 2012a) and stated competitive single impartial evolutionary procedures such as GA (Tang et al. 2012; Cui 2012), PSO (Tang et al. 2012; Cui 2012; Ramezanian et al. 2013), CAS (Cui 2012) due to its fewer adaptable limits and single separate base verbalized optimization mechanism with only mutation operation. The PID inside the AVR being the incharge of the optimal control contains differential, relative, and integral coefficients. Despite of many efforts an intelligent control system with

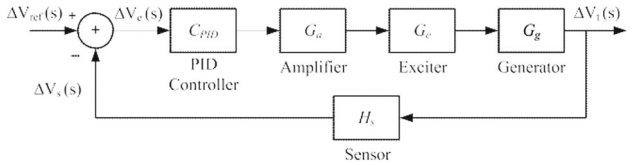

Fig. 1 AVR system with PID controller

optimum autonomy and effective mapping is far from being reached. In this situation, the present paper proposed the invention of a combined PSO and SFL approach to determine the optimal PID controller parameters and AVR system. This novel PSOFPID voltage is further used to get an AVR system. Also, the proposed algorithm could look for a high-quality solution effectively via full control system with improved transient response.

The rest of this paper is organized as follows. Division 2 elucidates the concept of AVR system modeling and optimization of the control parameters. Division 3 represents the concept of particle swarm optimization approach applied to PID parameters K_p, K_d and K_i those are automatically readjusted by PSO to keep the system error, $e(k)$ zero. Division 4 illustrates the proposed PSO for solving the PID controller parameter optimization. The utilization of Sugeno fuzzy system concepts for bringing out the PID control parameters under various operating conditions is presented in Division 5. Division 6 depicts the design methodology of fuzzy PID. Detailed simulation results are cleared up in Division 7. The analysis of results, validation and comparison with other findings are summarized in Division 8. The ending is given in Division 9.

2 Linearized model of An AVR system

For the stable electric power service it is essential to construct up a highly efficient and speedy AVR of the synchronous generator. Thus far, the analog PID inflammatory disease controller (PIDIDC) is generally applied for the AVR due to its ease and saving. However, the parameters of PIDIDCs cannot be tuned easily. Gaing (Gaing 2004) proposed a technique to determine such parameters by using a particle swarm optimization (PSO) algorithm. The AVR system model controlled by the PID controller is depicted in Fig. 1 with V_s the output voltage of sensor model, view the error voltage between V_s and the reference input voltage V_{ref} (S), V_r the amplified voltage by the electronic equipment model (amplifier model), V_f the output voltage by exciter mode, and V_t the output voltage of the generator. There are 5 models for the AVR system such as PID controller, electronic equipment (amplifier model), exciter, generator and (e) sensor. The transport use of each model is given by:

(i) PID controller model

$$G_s(s) = K_p + K_d\, s + \frac{K_i}{s} \tag{1}$$

where K_p, K_d, and K_i are the proportion coefficient, differential coefficient, and integral coefficient, respectively.

(ii) Amplifier model

$$\frac{V_r(s)}{V_e(s)} = \frac{K_A}{1 + \tau_A S} \tag{2}$$

where K_A is again and τ_A is a time constant.

(iii) Exciter model

$$\frac{V_F(s)}{V_R(s)} = \frac{K_E}{1 + \tau_E S} \tag{3}$$

where K_E is a gain and τ_E is a time constant.

(iv) Generator model

$$\frac{V_t(s)}{V_F(s)} = \frac{K_G}{1 + \tau_G S} \tag{4}$$

where B is again and τ_G is a time constant.

(v) Sensor model

$$\frac{V_S(s)}{V_t(s)} = \frac{K_R}{1 + \tau_R S} \tag{5}$$

where K_R is a gain and τ_R is a time constant. AVR system parameters considered in this work are; $K_a = 10.0$, $T_a = 0.1$, $K_e = 1.0$, $T_e = 0.4$, $B = 1.0$, $T_g = 1.0$, $K_s = 1.0$, $T_s = 0.01$ (Gaing 2004; Gozde and Taplamacioglu 2011; Panda et al. 2012; Tang et al. 2012; Pan and Das 2013; Sahib 2015). With these parameter values the closed-loop transfer function of the AVR system becomes:

$$G_{AVR} = \frac{\Delta V_t(s)}{\Delta V_{ref}(s)} = \frac{0.1s + 10}{0.0004s^4 + 0.045s^3 + 0.555s^2 + 1.51s + 11} \tag{6}$$

The transfer function of the AVR system (GAVR) has one zero at $z = -100$, two real poles at $s_1 = -98.82$ and $s_2 = -12.63$, and two complex poles at $s_{3,4} = -0.53 \pm 4.66i$. The GAVR can be approximated by canceling the zero at -100 with the pole at -98.82 to obtain ~GAVR. The unit step responses of GAVR and ~GAVR are shown in Fig. 2. It can be observed from Fig. 2 that the AVR system GAVR and its approximation ~GAVR are almost similar and possess an underdamped response with a steady-state amplitude

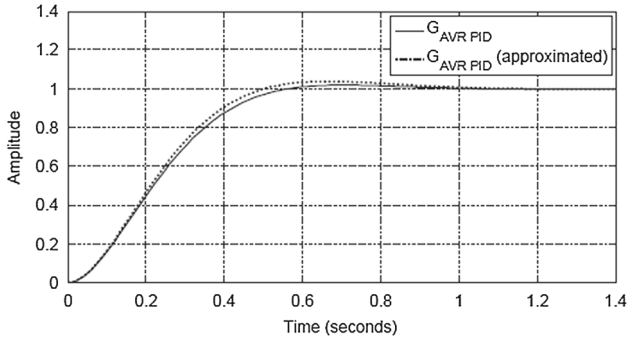

Fig. 2 Step response of the AVR system with PID controller

value of 0.909, peak amplitude of 1.5 (MP = 65.43%) at top = 0.75, t_r = 0.42 s, t = 6.97 s at which the response has worked down to 98% of the steady-state value.

2.1 Psychoanalysis of the AVR system with PID controller

The response of the AVR can be improved by utilizing a controller in the forward path capable of processing the voltage difference DVe(s) and producing a manipulated actuating signal. Normally, a PID controller is utilized for this project due to its simple construction. The PID controller combines three control actions related to the error signal in proportional, deferential, and integral manners and its transfer function are passed by:

$$C_{\mathrm{PID}} = K_{\mathrm{p}} + \frac{K_{\mathrm{i}}}{s} + sK_{\mathrm{d}} \tag{7}$$

where K_{p}, K_{i}, and K_{d} are the proportional, integral, and derivative gains, Fig. 1 depicts a block diagram of the AVR system with PID controller. The general transfer function of the AVR system controlled by a PID controller is made by

$$G_{\mathrm{AVR_{PID}}} = \frac{C_{\mathrm{PID}} G_{\mathrm{a}} G_{\mathrm{e}} G_{\mathrm{g}}}{(1 + C_{\mathrm{PID}} G_{\mathrm{a}} G_{\mathrm{e}} G_{\mathrm{g}} H_{\mathrm{s}})} \tag{8}$$

Substituting the transfer functions of the AVR system components listed in Table 1 with their parameters and the transfer function of the PID controller given by Eqs. (2) in (3) yields, the gist of the PID gain parameters on the overall AVR system can be examined by plotting the closed-loop zero-pole locus as a function of the PID gains. The zero-pole locus can be obtained when K_{p}, K_{i}, and K_{d} vary within the closed ranges $1 \le K_{\mathrm{p}} \le K_{\mathrm{p}}$ max, $0 \le K_{\mathrm{i}} \le K_{\mathrm{i}}$ max, and $0 \le K_{\mathrm{d}} \le K_{\mathrm{d}}$ max, respectively. The initial state of the zero-pole locus can be easily held by setting $K_{\mathrm{p}} = 1$, $K_{\mathrm{i}} = 0$, and $K_{\mathrm{d}} = 0$ in Eq. (4) and as a result the transport division of the

Table 1 The transfer functions of AVR components

Parts	Transfer function representation	Parameter out of range
Amplifier	$TF_{\mathrm{amplifier}} = K_a/1 + \tau_a s$	$10 \le K_a \le 40$ $0.02s \le \tau_a \le 1s$
Exciter	$G_e = TF_{\mathrm{exciter}} = K_e/1 + \tau_e s$	$1 \le K_e \le 10$ $0.4s \le \tau_e \le 1s$
Generator	$G_g = TF_{\mathrm{generator}} = K_g/1 + \tau_g s$	K_g depend on the load (0.7–1.0) $1s \le \tau_g \le 2s$
Sensor	$H_s = TF_{\mathrm{sensor}} = K_s/1 + \tau_s s$	$0.9 \le K_s \le 1.1$ $0.001s \le \tau_s \le 0.06s$

AVR system reduces to that given by Eq. (1) (without PID controller).

$$G_{\mathrm{AVR_{PID}}} = \frac{\Delta V_{\mathrm{t}}(s)}{\Delta V_{\mathrm{ref}}(s)} = \frac{46.52}{(s^2 + 9.8s + 46.52)} \tag{9}$$

The characteristic of the transient response of the AVR system is nearly interrelated to the position of the closed-loop poles. From the design viewpoint, the adaptation of the PID gains may move the closed-loop poles to a trusted position. Hence, with the employment of the zero-pole locus method, it is possible to find out the values of the PID gains that will get the damping ratio of the dominant closed-loop poles as prescribed. Even then, a multi-gain root locus is not an easygoing style to maintain and difficult to illustrate and plot along the complex plane. Instead, the problem of objective or cost function to tune the PID gains. For instance, Panda et al. (2012), proposed the simplified PSO algorithm to design a PID controller for the AVR system. By investigating the zero-pole map of the overall transfer function (the AVR system with the designed PID), given by (Panda et al. 2012).

One can observe that the objective of the PID controller is to compensate the effect of two poles in the AVR system at $s_1 = -2.11$ and $s_2 = -1.06$, thus the overall transfer function $G_{\mathrm{AVR_{PID}}}$ can be approximated to ~$G_{\mathrm{AVR_{PID}}}$. Figure 2 shows the step responses of $G_{\mathrm{AVR_{PID}}}$ and ~$G_{\mathrm{AVR_{PID}}}$. From Fig. 4, it is observable that the step response of the AVR system and its approximation has been improved when utilizing an optimal PID controller. This is evident through an improved value of rise time t_r = 0.343, settling time this = 0.516 s, maximum overshoot MP = 1.95%, and damping ratio ξ = 0.72. From the above analysis, it can be reasoned that the PID controller attempts to correct the effect of two poles of the AVR system. When the PID controller gain parameters are optimized, the overall transfer function is approximately reduced from fourth to a simple second-order scheme. Nevertheless, in a second-order system, the maximum overshoot and the rise time of the unit step response conflict with each other. Thus,

the advance of the AVR system response achieved by the conventional PID controller is a compromise between maximum overshoot and rise time. The transfer functions of the AVR components are identified in Table 1.

The best selection of PID controller parameters is of the essence for the satisfactory operation of the organization. Thus, the problem of PID controller parameter selection is fixed as an optimization problem wherein the objective part is given by:

$$\mathrm{Min}F(K_\mathrm{d}, K_\mathrm{p}, K_\mathrm{i}) = (1 - e^{-\beta})(O_\mathrm{sh} + E_\mathrm{ss}) + e^{-\beta}(t_\mathrm{s} - t_\mathrm{r}) \tag{10}$$

where $\mathrm{Min}F(K_\mathrm{d}, K_\mathrm{p}, K_\mathrm{i})$ uses a combination of transient response counting rise time, overshoot, settling time and steady-state error.

By choosing the suitable value of the weighting factor, the presentation principle can be formed to please the designer requirements. The above optimization problem is subjected to the following restrictions. The presentation standard $W(k)$ can satisfy the fashionable requirements using the weighting β factor value. We can set β to be larger than 0.7 to reduce the overshoot and steady-state error. On the other hand, we can set β to reduce less than 0.7 to reduce the rise time, settling time and settling time. In this paper, β is set in the range of 0.8–1.5.

$$K_\mathrm{p}^{\min} \le K_\mathrm{p} \le K_\mathrm{p}^{\max}, K_\mathrm{i}^{\min} \le K_\mathrm{i} \le K_\mathrm{i}^{\max}, \quad K_\mathrm{d}^{\min} \le K_\mathrm{d} \le K_\mathrm{d}^{\max} \tag{11}$$

Here, PSO is applied to the above optimization problem to search for the optimum value of the controller parameters. The detail of proposed PSO is depicted hereunder.

3 A particle swarm optimization approach

This paper proposed Particle Swarm Optimization Approach to choice a suitable controller parameter set $K = (K_\mathrm{p}, K_\mathrm{d}, K_\mathrm{i})$ of the PID controller. A PID controller using the particle swarm optimization approach (PSO) algorithm was industrialized to advance the step transient response of AVR of a generator. It was also called the PSO-PID controller. The PSO algorithm was mainly applied to control three optimum controller parameters, and, such that the controlled system could acquire a good step response output.

3.1 Individual string definition

To use the PSO technique for searching the controller parameters, we apply the "individual" to substitute the "particle" and the "population" to substitute the "group" in this report. We defined three controller parameters K_p, K_i, and K_d, to install a separate K by $K = [K_\mathrm{p}, K_\mathrm{i}, K_\mathrm{d}]$; thus, there are three members in a separate. These members are allocated as real values. If there are individuals in a population, then the dimension of a population is $nx3$. The matrix representation in a population is as follows.

3.2 Evaluation function definition

In the interim, we defined the assessment function given in (12) as the assessed value of each separate in population. The assessment function f is a reciprocal of the presentation standard $W(k)$ as in (10). It implies the lesser $W(k)$ the value of distinct k, the advanced its assessment value

$$F = \frac{1}{W(K)} \tag{12}$$

Hence, as to limit the assessed value of each separate of the population within a reasonable range, the Routh–Hurwitz criterion must be active to test the closed-loop system stability before assessing the assessment value of a separate. If the separate satisfies the Routh–Hurwitz stability test applied to the characteristic equation of the scheme, and thus it is a feasible separate and the value of w (k) is small. In the conflicting case, $w(k)$ the value of the separate is penalized with a really large positive constant.

3.3 Proposed PSO-PID controller

This paper gifts a PSO-PID controller for penetrating the best or near best controller parameters K_p, K_i, and K_d, with the PSO algorithm. Each individual contains three members K_p, K_i, and K_d. The matrix representation of the initial population is reported in Sect. 3.1. Its dimension is $nx3$. The penetrating events of the proposed PSO-PID controller were exposed as below.

Step 1 Stipulate the lower and upper bounds of the three controller parameters and reset arbitrarily the individuals of the population, including searching points, velocities, s, and.

Step 2 For each initial separate of the population, employment the Routh–Hurwitz criterion to prove

The closed-loop system constancy and calculate the values of the form creation in the time domain, namely MP, E_ss, t_r, and t_s.

Step 3 Calculate the measured value of each separately in the population using the assessment function given by (11).

Step 4 Compare each person's assessment value with its best. The best assessed value between them is denoted as best.

Step 5 Modify the member velocity v of each separate K according to (13)

$$v_{jxg}^{(t+1)} = w.v_j^{(t)} + c_j^{*}\text{rand}()^{*}\left(p\text{best}_{j,g} - k_{j,g}^{(t)}\right) + c_2^{*}\text{Rand}()^{*}\left(g\text{best}_g - k_{j,g}^{(t)}\right)$$
$$J = 1, 2 \ldots n,$$
$$g = 1, 2 \ldots, 3 \tag{13}$$

where the value of w is set of (14). As originally industrialized, we often decreases linearly from about 0.9 to 0.4 during a foot race. In universal, the inertia weight is set according to the following equation:

$$w = w_{\max} - \frac{w_{\max - w_{\min}}}{iter_{\max}} * \text{iter} \tag{14}$$

When g is 1, $v_{j,1}$ represents the change in speed of the K_p controller parameter.

When is 2, represents the change in velocity of the ki controller parameter.

Step 6 If, $v_{j,g}^{(t+1)} > V_g^{\max}$, then $v_{j,g}^{(t+1)} = V_g^{\max}$ then If $v_{j,g}^{(t+1)} < V_g^{min}, then v_{j,g}^{(t+1)} = V_g^{min}$.

Step 7 Modify the member position of each separate according to (15)

$$k_{j,g}^{(t+1)} = k_{j,g}^{(t)} + v_{j,g}^{(t+1)}, k_{j,g}^{\min} \le k_{j,g}^{(t+1)} \le k_g^{\max} \tag{15}$$

where $k_g^{\min}$ and $k_g^{\max}$ represent the lower and upper bounds, respectively, of members of the individual K. For example, when g is 1, the lower and upper bounds of the K_p controller parameter are $k_\text{p}^{\min}$ and $k_\text{p}^{\max}$, respectively.

Step 8 If the number of iterations reaches the upper boundary, then carry on to Step 9. Otherwise, merely continue to Step 2.

Step 9 The separate that generates the latest is a best controller parameter.

4 PSO implantation

The optimal PID controller parameters are achieved by applying PSO, which involved two major aspects:

(i) Variables representation and
(ii) Determine the fitness function

4.1 Variable representation

For PID controller tuning, candidate solutions in the genetic population are represented. The elements of the solution consisted of the variables such as the integral gain (K_i), proportional gain (K_p) and derivative gain (K_d) which are reprinted by point number in the proposed PSO population. Using this representation, an individual in the proposed PSO is computed to achieve the optimal PID gain. Interestingly, the computer memory requirement to store the population is remarkably reduced due to the direct representation of the result variables. The value of the parameter set that is obtained from PSO to obtain the optimal value of PID controller parameter. This optimum value is essential to design a fuzzy PID controller for the thematic factory operation of AVR system.

4.2 Fitness function

It is defined as the nonnegative figure of value to be maximized so that the performance of each individual in the population can be evaluated. The fitness function is the mutuality of the presentation criterion $F(K_\text{d}, K_\text{p}, K_\text{i})$ given in Eq. (10). Hence, the minimization of performance criteria is transformed into a fitness function to be maximized as,

$$\text{Fitness} = \frac{k}{F\left(K_\text{d}, K_\text{p}, K_\text{i}\right) * \text{ITAE}} \tag{16}$$

where k is constant, ITAE is an integral of time multiplied by the absolute error value, K_p, K_i, and K_d are the proportional, integral, and derivative gains of PID controller. This is applied to amplify $1/F$ (usually minor) so that the fitness value of the chromosome occurs in a broader scope in a wider range (Devaraj and Selvabala 2009; Gaing 2004).

5 Sugeno fuzzy model

Devaraj and Selvabala (2009) and Al Gizi et al. (2015) the fuzzy rule was expressed equally:

$$\text{If } x \text{ is } A \text{ and } y \text{ is } B \text{ then } z = f(x, y) \tag{17}$$

where A and B are the fuzzy sets in the antecedent, x and y are input variables and f (x, y) is a crisp function in the sequent. Each variation in the fuzzy set is represented by suitable membership functions. The nub of the fuzzy logic system is formed by a lot of such rules. For an accurate input signal condition, the fuzzy system defined the conventions to be fired and then weighed on the efficient output in two steps. Foremost, the minimum of the membership function's input (w_i) was obtained for each ruler, where this value is reckoned as the firing value for a particular pattern or a particular rule. Second, the overall turnout was calculated by a

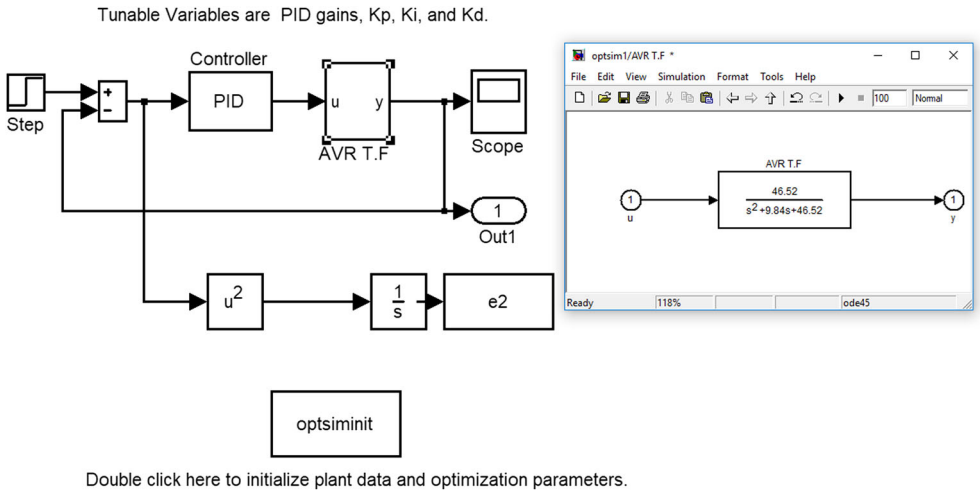

Fig. 3 A thematic factory operation of AVR system with B from 0.8 to 1.5 and no. of birds from 50 TO 150

weighted average of individual rule outputs given by Devaraj and Selvabala (2009):

$$z = \frac{\sum_{i=1}^{M} w_i z_i}{\sum_{i=1}^{M} w_i} \tag{18}$$

The PID controller parameters under various operating conditions were set by the Sugeno fuzzy system.

6 Design of a particle swarm optimization, fuzzy PID controller based on (β and no. of birds) and SF model

Optimal PID parameters during real-time operation are obtained from Sugeno fuzzy logic example. B and no. birds are the inputs to the fuzzy model and the values of K_p, K_d and K_i are the outputs. Four fuzzy sets, namely, 'Very low (VL)', 'tiny, low (TL)', 'low (L)', 'medium low (ML)', 'medium high (MH)', 'high (H)', 'very high (VH)'and 'Extra high (EH)', are defined for the variable B. Also, the fuzzy sets defined for the variable no. of birds are 'low (L)', 'medium (M)', 'high (H)'. All these parameters are linked up with overlapping triangular membership functions. To formulate the fuzzy rule table the value of B is varied from 0.8 to 1.5 in steps of 0.1 and no. of birds varies from 50 to 150 in steps of 50. For every combination of B and no. of birds the proposed PSO is applied to obtain the optimal values of K_P, K_d and K_i in each time. The values of B and no. of birds are confined by the load ($0.8 \leq B \leq 1.5$) and $50 \leq$ no. of birds ≤ 150). For these values of B and no. of dames, the optimal value of K_p, K_d and K_i can be calculated. Our take $B = 0.7$ and no. of birds $= 1$ a for a thematic factory operation of the AVR system shown in Fig. 3. The obtained values of parameters K_p, K_d and K_i are 0.2095, 0.1516 and -0.0446, respectively. These are obtained from direct tuning of PSO to realize the optimal tuning of proportional–integral–derivative controller parameter. It is demonstrated that these values are necessary for designing the novel fuzzy controller of the AVR system by the fuzzy rule table and the FIS editor Sugeno inference system.

The fuzzy rule table expressed for K_p, K_d and K_i uses the above method is summarized in Table 2(a–c), correspondingly. The computed fuzzy rule table is further employed to design a PSOFPID controller by FIS editor Sugeno inference system. Depending on the initialization (FIS editor), the inputs of the fuzzy logic controller are B, no. of birds and the outputs are K_p, K_d and K_i. The arrangement with three output fuzzy logic controllers namely K_p, K_d and K_i with rule viewer are set in which the accountant receives two inputs B, no. of birds and the input has fuzzy set associated with it. The output has 72 fuzzy set rules for K_p, K_d and K_i, and the rule and surface viewer of novel PSOFPID controller is described in Fig. 4. The best effect is reached by following command parameters for PSO: size of the swarm "no of birds ($n = 50, 100, 150$)", Maximum number of "*bird steps* (50)", dimension of the problem (2), PSO parameter $C2$, $C1$ (1.5, 0.12), $M_p = 0.045$, $E_{ss} = 0.950$, $t's = 0.8645$, $t_r = 0.2138$, ITAE $= 1$, Val $=$ ITAE,

$w = ((1 - \exp(-B)) * (O_{sh} + E_{ss}) + \exp(-B) * (t_s - t_r) *$ val). The PSO took 1:17:27.96 s to reach the optimal solution.

7 Simulation and discussion results

The MATLAB-Simulink model of Electrical Power Generation and Distribution System along with PSOFPID controller is displayed in Figs. 5, 6 shows the novel fuzzy PID controller (PSOFPID). The AC power–frequency is constant and depends on the engine speed control by GA. The generator

Table 2 Sugeno fuzzy rule

	Very low	Tiny, low	Low	Medium low	Medium high	High	Very high	Extra high
B (bate) No. of birds *n*	0.8	0.9	1	1.1	1.2	1.3	1.4	1.5
(a) For proportional gain K_p								
Low (50)	0.2095	−0.0648	0.4213	−0.048	0.4322	−0.0688	−0.0645	−0.0298
Medium (100)	0.1011	−0.0908	−0.0761	0.0138	−0.0263	−0.0688	0.0854	0.4622
High (150)	0.1263	−0.1069	−0.0086	−0.0422	−0.0586	1.0199	−0.0917	−0.0177
(b) For derivative gain K_d								
Low (50)	0.1516	−0.0586	−0.0786	−0.04	0.0666	−0.0654	−0.0601	−0.0296
Medium (100)	0.0919	−0.1386	0.3331	−0.0087	−0.1534	−0.0654	−0.0871	−0.1319
High (150)	−0.1206	−0.1134	−0.0064	1.0494	−0.0335	−0.1589	−0.0852	−0.0143
(c) For integral gain K_i								
Low (50)	−0.0446	−0.0475	−0.0817	−0.038	−0.0204	−0.0718	−0.0575	−0.0287
Medium (100)	−0.007	−0.0917	−0.071	−0.0105	−0.0254	−0.0718	−0.0847	−0.147
High (150)	−0.1297	−0.1096	−0.0064	−0.0356	−0.0279	−0.1541	−0.0905	−0.0143

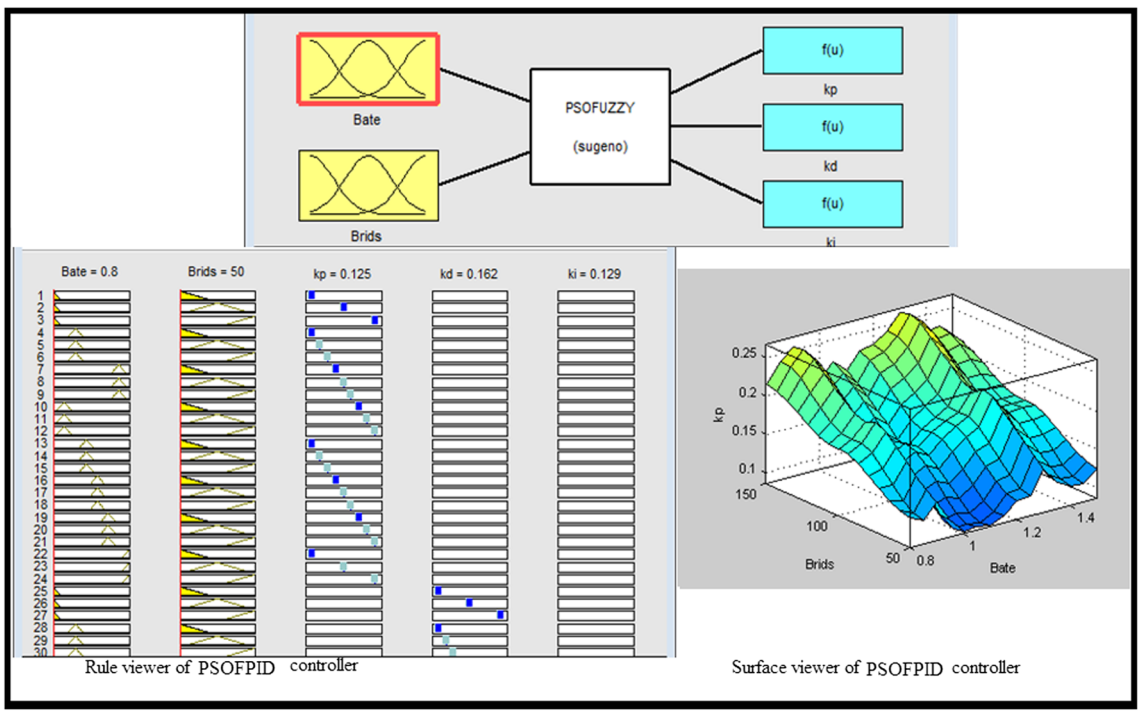

Fig. 4 Rule and surface viewer of PSOFPID controller

mechanical drive is modeled by speed control of an induction motor system which provides AC generator the mechanical constant speed (3000 RPM). The optimization problems are solved by GA because of its realization as an efficacious and effective technique of speed control. Compared with other optimization techniques, such as random search method and simulating annealing, GA is efficient in avoiding local minima which is an important issue for nonlinear

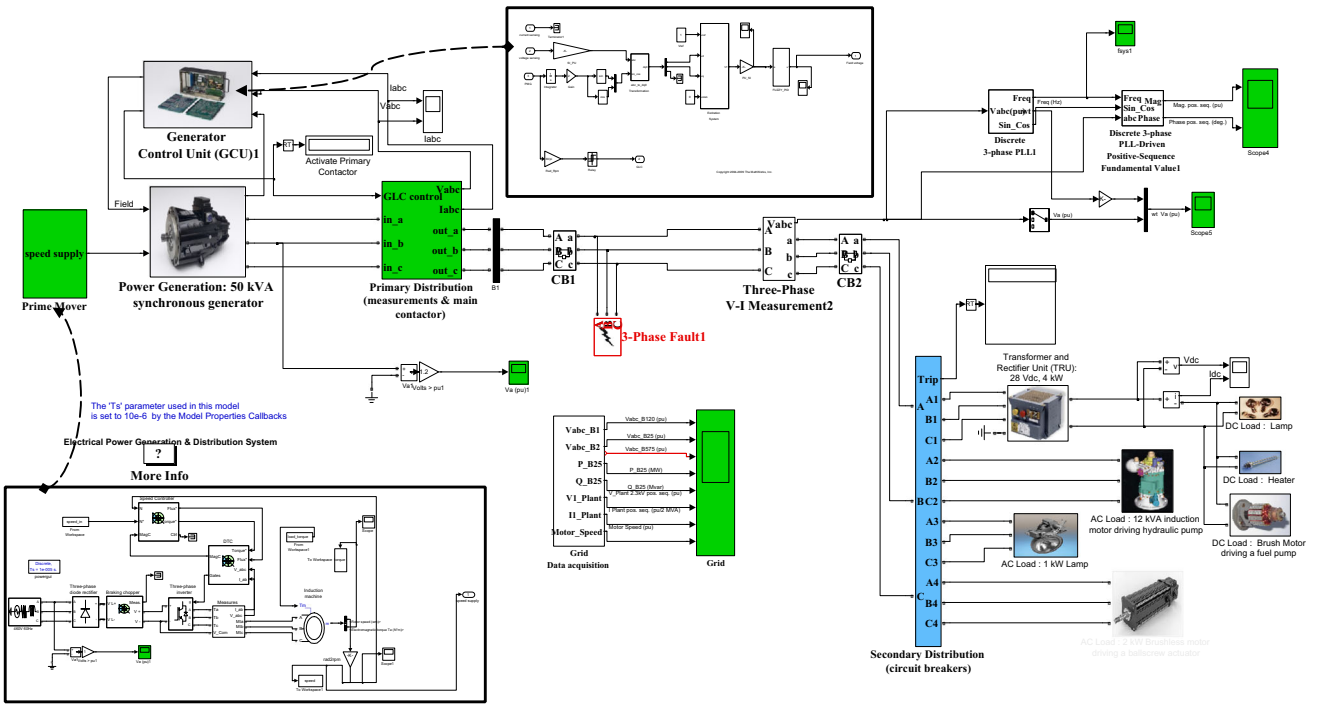

Fig. 5 The MATLAB-Simulink model of electrical power generation system along with fuzzy PID controller PSOFPID

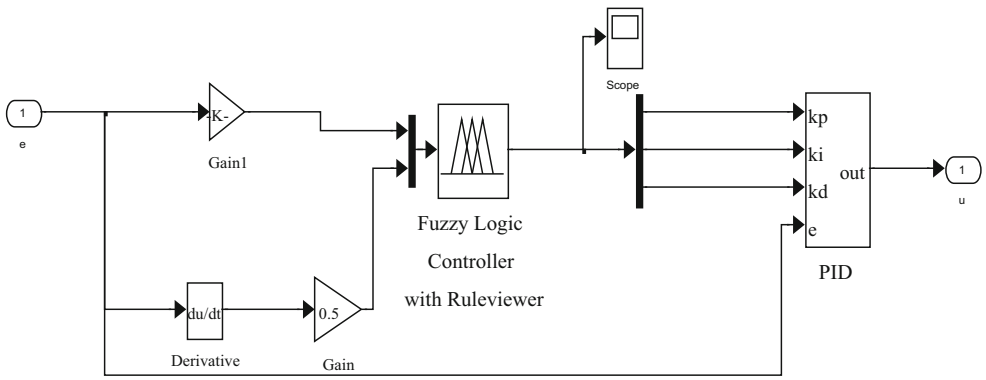

Fig. 6 Novel fuzzy PID controller PSOFPID

systems Arulmozhiyal and Baskaran (2009). GA begins with an initialization of the system data and population, conducting a number of chromosomes where everyone represents a solution of the problem. The performance of the GA is assessed by a fitness function. The diligence of the GA*'s* main stages, including selection, crossing over and mutation allow the institution of raw individuals, which may be more dependable than their parental counterparts. This algorithm is iterated for many generations and finally breaks up after reaching the optimal solution of individuals (optimum speed control).

The AC generator is composed of a modified version of the simplified synchronous machine. The mechanical input of the modified machine of 50 kW is the engine speed. AVR consisting of PSOFPID controller and exciter regulates the terminal voltage of the generator to 400 V line to line under different operating conditions. Whereas, the primary delivery system is calm of three current and electric potential sensors. A 3-phase contractor controlled by the generator control unit is likewise utilized. A parasitic resistive load is needed to ward off the numerical fluctuations.

In sum, a secondary power delivery system signified by four circuit breakers with adaptable current trip is made up. AC loads are supplied from 4 kW modifier and the rectifier unit (7 Vdc). A 12 kW induction machine (motor driving a pump), 1 kW resistive load (lamps) and 3 HP simplified (using an average value inverter) brushless DC drive (motor driving a ball screw actuator) are worked in. The DC loads

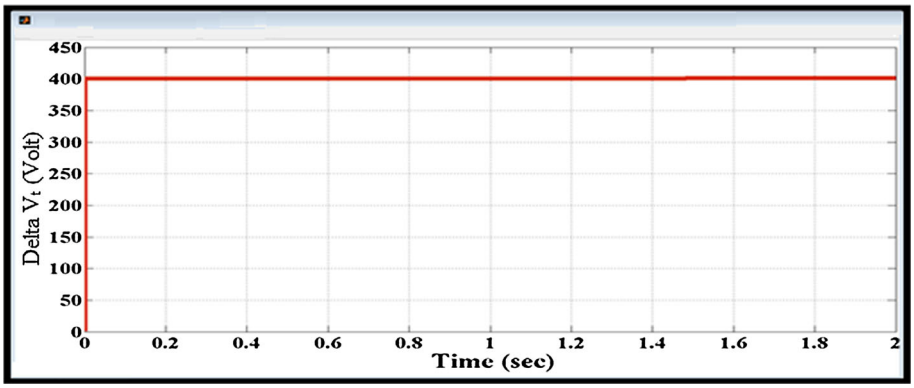

Fig. 7 Terminal voltage response of excitation system with novel controller PSOFPID

(a)

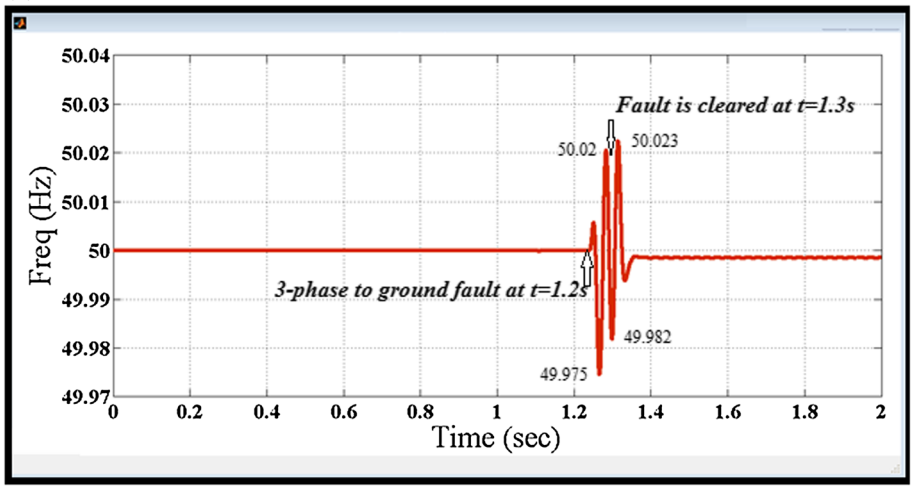

(b)

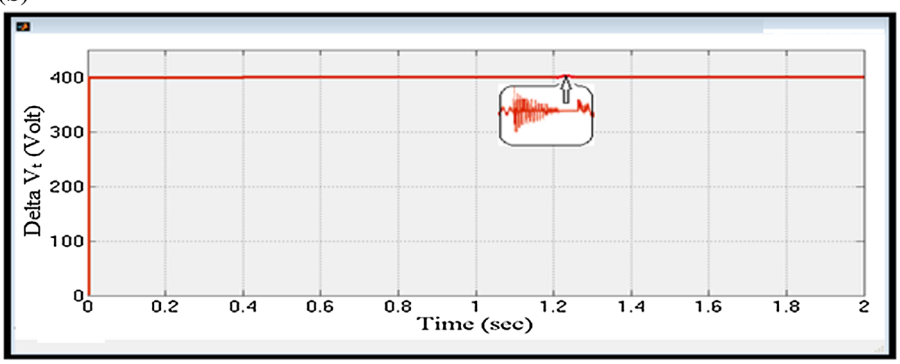

Fig. 8 The terminal voltage and frequency response under three phases to ground fault with PSOFPID controller

comprised of two resistive loads (heater and lamp) and a 300 W DC brush motor (motor driving a fuel pump).

The suitability of the proposed access to receive the optimal PID gains during system real-time operation is clearly shown. Block measures the frequency, whereas the PLL drives two measurement blocks taking into account the varying frequency: one block computes the fundamental value of the positive-sequence load voltage and the other one computes the load active and responsive powers.

In summing up, the block three-phase fault to program fault (short-circuit) between any phase and dry land for test stability of system are introduced. The system response to new fuzzy PID controller designed by the Sugeno fuzzy model rule that obtained from PSO is displayed in Fig. 7. Our proposed method yields better performance in the rise time, peak overshoot and the steady-state error. The reactions observed from the present controller do not possess a slight overshoot as shown in Figs. 8 and 9.

We verify that the PSOFPID controller has more honest performance in comparison to other controllers. To test the performance of the AVR system with novel fuzzy PID controller under severe disturbance, a three-phase fault is

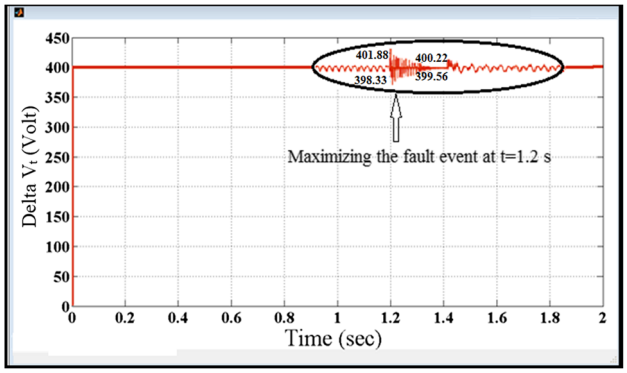

Fig. 9 The response of the terminal voltage under three phases to ground fault with PSOFPID controller

applied at the generator terminal and the response of the system is supervised. A three-phase to ground fault on the 400 V Busbar occurred at $t = 1.2$ s in which the scope block clearly reveals the tracking of the system frequency change by PLL. The frequency of the system at moment of fault swing between 49.975 and 50.02 Hz. Shedding light on the error at $t = 1.3$ s makes the frequency to swing between 49.982 and 50.023 Hz and then extends to the steady-state value of 49.9997 Hz at $t = 1.38$ s. In sum, at $t = 1.2$ is when three-phase to ground fault occurs on the same Busbar (400 V) the system voltage at moment of fault swings between 398.33069 and 401.879839 V. Upon solving the error at $t = 1.3$ s is the voltage swings between 399.567889 and 400.22346 V before reaching the steady-state value of 400 V at t = 1.36 s is as shown in Fig. 8a, b. Figure 9 represents the response of the terminal voltage under 3 phase ground fault with PSOFPID controller.

The trustworthiness of the proposed PID control parameters and the AVR system model is validated by comparing our results with other works. The reaction of the system with a novel fuzzy PID controller is extremely sensitive to tiny change (0.005) as depicted in Fig. 10. We find that our approach (PSOFPID controller) results minimum values of rise time, steady-state error, less settling time, shorter convergence time and tiny overshoot in comparison with the result obtained using LQR (Gwo-Ruey and Rey-Chue 2004), RAG and binary-coded GA (Devaraj and Selvabala 2009) as displayed in Table 3.

Figure 11 shows the system response for above contingency with the newly proposed PSOFPID controller. It can be observed that the PSOFPID controller is able to bottle up the oscillation in the terminal voltage and better the transient response (0.001) and provide good damping characteristics.

8 The analysis of results, validation and comparison with other determinations

The dependability of the proposed PSOFPID controller parameters and the AVR system is checked and compared with existing literatures as mentioned before (Vural and Bayindir 2012; Shamisa et al. 2008; Shivakumar et al. 2010; Wahab and Mohamed 2010). The reaction of the system with a new fuzzy PID controller is highly sensitive to a very small change (0.005) (Mustafa and Al Gizi 2013; Mustafa and Al Gizi 2013) as shown in Fig. 10. The proposed methodology provides good performance in the rise time, peak overshoot and the steady-state error. Our simulation shows that the PSOFPID performs better than the conventional controller such as LQR (Gwo-Ruey and Rey-Chue 2004), RAG and binary-coded GA (Devaraj and Selvabala 2009) by keeping the system error approach to zero. By comparing these results, it is found that the proposed PSOFPID controller has minimum settling time values, less rise time, overshoot and steady-state error (0.0009, 0.0008, 0, 0.0025) in comparison with other calculation following LQR, PSO, RAG and binary-coded GA as summarized in Table 3.

The novel PSOFPID controller improved the transient response (0.001) by minimizing the swing in terminal voltage between the up and down swing to 0.0088739 and saved the system stable as evidenced in Fig. 12. This is good agreement with the report of Devaraj and Selvabala (2009) and Wong et al. (2009). Moreover, PSOFPID is able to suppress the

Fig. 10 High sensitivity voltages to tiny change (0.005)

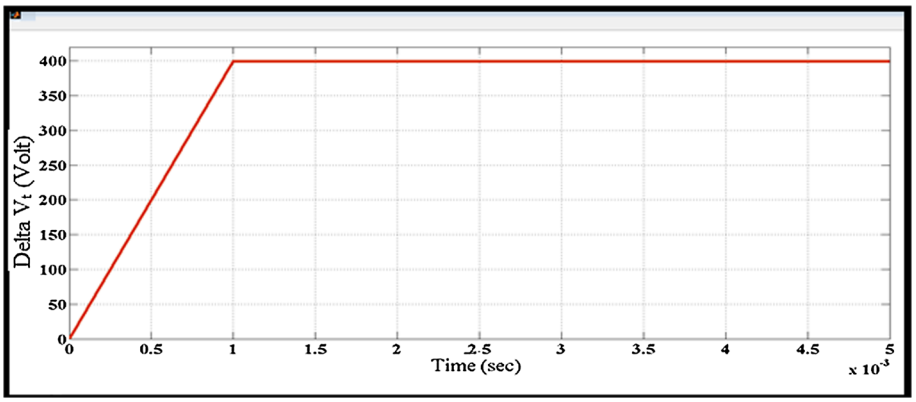

Table 3 Comparison between the proposed method and the previous methods

Method	T_s (S)	T_r (S)	O_{sh}	E_{ss} (10 − 5)
LQR (Gwo-Ruey and Rey-Chue 2004)	2.3354	0.5004	0.3605	15.007
Binary-coded GA	1.708	0.8093	0.0586	8.841
RGA (Devaraj and Selvabala 2009)	1.2682	1.0668	0.0004	4.3386
RBF tuning by GA	1.3766	1.0024	0.00168	5.365
RBF tuning binary-coded GA	1.4050	0.9405	0.0085	6.2490
RBF tuning by RGA	1.3849	0.9522	0.00167	5.8305
PSO (Gaing 2004)	0.457	0.3070	0.44	0
Proposed method PSOFPID	0.001	0.0008	0	0.0025

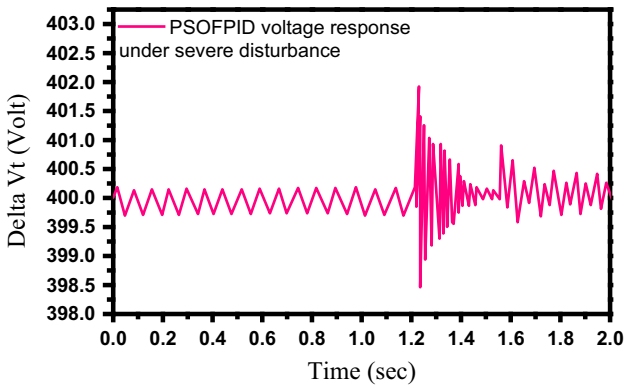

Fig. 11 Terminal voltage response under three phases to ground fault

oscillation in the terminal voltage and provide good damping characteristics. The present technique automatically avoids the problem of over fitting, which adversely affects many optimizations and learning algorithms.

By directing the combined PSO and Sugeno fuzzy logic with the normalized inputs the training performance reached the destination perfection. As earlier, the best combination of B and no. of birds is applied to obtain the values of K_p, K_d and K_i. The PSO had optimize the parameters of PID to reach the optimum parameters additional rapidly, so that the PSOFPID characteristics obtained are better than fuzzy PID and PSO-PID (Devaraj and Selvabala 2009; Rahimian and Raahemifar 2011). These data are authentic, because the solution of the fuzzy rule table test response acquires high sensitivity and the system error very limited. The system response to novel PSO Sugeno fuzzy PID (PSOFPID) controller is found to possess

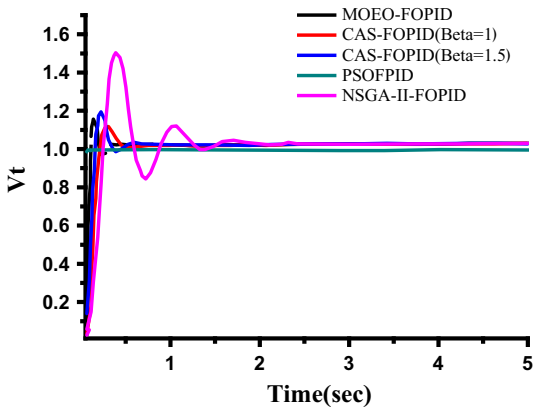

Fig. 12 Comparison with PSOFPID data with other methods

the minimum settling time values, rise time, overshoot and steady-state error compared to other existing methods. Our PSOFPID controller tracks the set point with small oscillation because of the speed prime mover at the outset is a variable and after that reached the rated speed 3000 r.p.m. The induced voltage at the start is higher than the rated voltage according to Faraday's Law (Barnes and Maekawa 2007). Therefore, the numerical convergence can easily be reached in our newly proposed fuzzy PID.

The transient response of a practical control system often exhibits damped oscillations before reaching steady state. Holdup time: The time is necessitated for the response reach 50% of the final value. Rise Time: Increase time is defined as the period for the waveform to go from 0.1 to 0.9 of its last value. Settling Time: Settling time is defined as the time for the response to reach, and stay within, 2% (or 5%) of its final value. Peak Time: The time required to reach the first, or maximum, peak. Percent Overshoot: The amount that the waveform overshoots the steady-state, or final, value at the peak time, extracted as a percentage of the steady-state value. From Fig. 13 illustrated transient response specifications above, we calculate the (1) delay time TD, (2) rise time t_r, (3) peak time t_p, (4) maximum overshoots MP, (5) settling time outs for signal shown in Fig. 13.

The public presentation of the proposed PSOFPID was compared (Table 3) with other connected system such as NSGA-II-FOPID, GA-FOPID, PSO-FOPID, CAS-FOPID and competitive single-objective evolutionary algorithms-based FOPID controllers. The terminal voltage step response of AVR system is depicted in Fig. 11. The proposed PSOFPID was found to be more robust and better than those reported NSGA-II-FOPID, GA-FOPID (Pan and Das 2012a), PSO-FOPID (Pan and Das 2012a), CAS-FOPID with β¼ = 1 and β¼ = 1.5 (Pan and Das 2012a, 2013) under the uncertainty of amplifier model parameters as shown in Fig. 12. Yet, from the position of technology design and system operation the performance of PSOFPID was accepted by engineers under

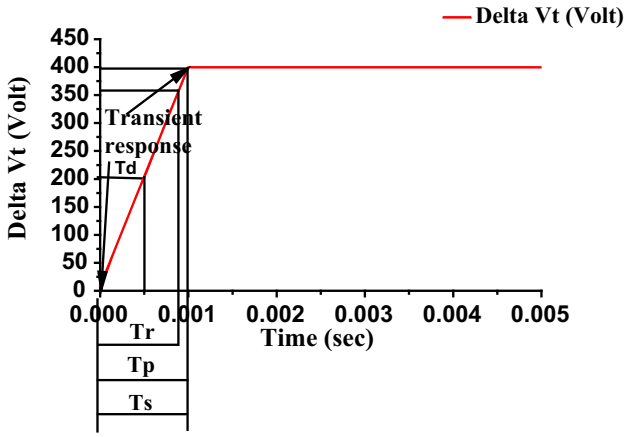

Fig. 13 Transnet response specifications

the variance of parameters B and no. of birds are enlisted in Table 1. Figure 12 demonstrated the terminal voltages step response of the AVR system with MOEO-FOPID controller when K_A was varied from K_g depending on the load (0.7–1.0), and τ_A (1.0–2.0). Understandably, as the value of parameter K_a was increased, the overshoot (MP) was also increased, but the rising time (t_r) and settling time (this) became shorter; and the steady-state error (E_{ss}) appeared smaller. A comparison with other calculation revealed that the proposed PSOFPID controller achieved minimal settling time, short rise time, and overshoot (0.001, 0.0008, 0). In short, the developed PSOFPID controller can be viewed as robust for the uncertainty of amplifier model parameter within the range defined (Table 4).

9 Conclusion

We assumed a blended approach of PSO and SFL to achieve the optimal PID controller parameters in AVR system. In this proposed system, PSO is used to enhance the PID parameters to design Sugeno fuzzy PID controller tuned by generator parameter (β, no of birds in). The developed algorithm provided a high-quality solution effectively and offered full control of the electromotive force of the proposed system compared with other existing art of the techniques. The PSOFPID controllers are capable of bottling up the oscillation in the terminal voltage and better transient response providing good damping characteristics. Our approach on PSOFPID controller produce ultra-short rise time, less steady-state error, less settling time, shorter convergence time and tiny overshoot (0.001, 0.0008, 0) in comparison other conventional methods such as NSGA-II-FOPID, GA-FOPID, PSO-FOPID, CAS-FOPID with β¼1 and β¼1.5 under the uncertainty of amplifier model parameters.

Table 4 Comparative performance of different evolutionary algorithms

Algorithm M_p (%)	M_p (%)	t_r (s)	t_s (s)	E_{ss}
GA-FOPID (Sahib 2015)	17.6371	0.12	0.26	4.05E−04
PSO-FOPID (Sahib 2015)	10.46691	0.12	0.24	4.63E−04
CAS-FOPID (β¼1) (Sahib 2015)	9.079521	0.17	0.32	2.35E−04
CAS-FOPID (β¼1.5) (Sahib 2015)	8.941498	0.17	0.36	1.89E−04
NSGA-II-FOPID (Pan and Das 2012a, b)	46.71605	0.2	1.12	6.92E−0
MOEO-FOPID (Zeng et al. 2015)	14.07733	0.07	0.23	2.98E−05
Proposed method PSOFPID	0	0.0008	0.001	0.0000
Parameterization sets	The optimum PID parameters for real-time operation are obtained by developing surgeon fuzzy logic example. Here, B and *no. birds are the inputs and* K_p, K_d *and* K_i *are the end products.* Eight and six fuzzy sets are set for the variable β and no. of birds, respectively			
Pretense Solutions	The response of the system with a new fuzzy PID controller is highly sensitive to a very small change (0.005)			
	The proposed methodology achieves good performance in the rise time, peak overshoot and the steady-state error			
	The novel PSOFPID controller improved the transient response by minimizing the swing in terminal voltage between the up and down swing, wave and kept the system stable as reported by Devaraj and Selvabala (2009), Wong et al. (2009), Madinehi et al. (2011) and Rahimian and Raahemifar (2011)			
Standardize deviation steady stat error	(400 − 399)/400 = 0.0025			

Acknowledgements Abdullah is thankful to Dr. S. K. Ghoshal for many valuable hints and critical interpretations of the holograph.

Compliance with ethical standards

Conflict of interest Author Abdullah declares that he has no conflict of interest.

Ethical approval This article does not contain any studies with human participants or animals performed by any of the authors.

References

Al Gizi AJ, Mustafa M, Al-geelani NA, Alsaedi MA (2015) Sugeno fuzzy PID tuning, by genetic-neutral for AVR in electrical power generation. Appl Soft Comput 28:226–236

Al-geelani NA, Afendi M, Piah M, Shaddad RQ (2012) Characterization of acoustic signals due to surface discharges on H.V. glass insulators using wavelet radial basis function neural networks. Appl Soft Comput 7(2):1327–1338

Arulmozhiyal R (2012) Design and implementation of fuzzy PID controller for BLDC motor using FPGA. In: IEEE international conference on power electronics, drives and energy systems (PEDES), 2012, 16–19 Dec 2012, pp 1–6

Arulmozhiyal R, Baskaran K (2009) Speed control of induction motor using fuzzy PI and optimized using GA. Int J Recent Trends Eng 2(5)

Arulmozhiyal R, Kandiban R (2012) Design of fuzzy PID controller for brushless DC motor. In: 2012 international conference on computer communication and informatics (ICCCI), 10–12 Jan 2012, pp 1–7

Barnes S, Maekawa S (2007) Generalization of Faraday's law to include nonconservative spin forces. Phys Rev Lett 98(24):246601

Chatterjee A, Ghoshal S, Mukherjee V (2011) Chaotic ant swarm optimization for fuzzy-based tuning of power system stabilizer. Int J Electr Power Energy Syst 33(3):657–672

Chen W, Xing M, Fang K (2012) A PLC-based fuzzy PID controller for pressure control in Coke-oven. In: 2012 31st Chinese control conference (CCC), 25–27 July 2012, pp 4754–4758

Chen Z, Yuan X, Ji B, Wang P, Tian H (2014) Design of a fractional order PID controller for hydraulic turbine regulating system using chaotic non-dominated sorting genetic algorithm II. Energy Convers Manag 84:390–404

Cui M (2012) Low carbon dispatch of distribution network containing microgrid using chaotic ant swarm. In: 2012 international conference on control engineering and communication technology (ICCECT), IEEE, pp 818–821

Devaraj D, Selvabala B (2009) Real-coded genetic algorithm and fuzzy logic approach for real-time tuning of proportional-integral—derivative controller in automatic voltage regulator system. Gener Transm Distrib IET 3(7):641–649. https://doi.org/10.1049/iet-gtd.2008.0287

Gaing ZL (2004) A particle swarm optimization approach for optimum design of PID controller in AVR system. IEEE Trans Energy Convers 19(2):384–391. https://doi.org/10.1109/TEC.2003.821821

Gozde H, Taplamacioglu MC (2011) Comparative performance analysis of artificial bee colony algorithm for automatic voltage regulator (AVR) system. J Frankl Inst 348(8):1927–1946. https://doi.org/10.1016/j.jfranklin.2011.05.012

Guerrero JM, Chandorkar M, Lee T-L, Loh PC (2013) Advanced control architectures for intelligent microgrids, part I: decentralized and hierarchical control. IEEE Trans Ind Electron 60(4):1254–1262

Gwo-Ruey Y, Rey-Chue H (2004) Optimal PID speed control of brush less DC motors using LQR approach. In: 2004 IEEE international conference on systems, man and cybernetics, 10–13 Oct 2004, vol 1, pp 473–478

Higgins N, Vyatkin V, Nair N-KC, Schwarz K (2011) Distributed power system automation with IEC 61850, IEC 61499, and intelligent control. IEEE Trans Syst Man Cybern C (Appl Rev) 41(1):81–92

Jiang J (1995) Design of an optimal robust governor for hydraulic turbine generating units. IEEE Trans Energy Convers 10(1):188–194

Jinwook K, Oh-Kyu C, Lee JS (2012) Design and stability analysis of TSK-type full-scale fuzzy PID controllers. In: 2012 IEEE international conference on fuzzy systems (FUZZ-IEEE), 10–15 June 2012, pp 1–8

Madinehi N, Shaloudegi K, Abedi M, Abyaneh HA (2011) Optimum design of PID controller in AVR system using intelligent methods. Power Tech, 2011 IEEE Trondheim. IEEE, 19–23 June 2011, pp 1–6

Man-chen X, Ling-long W (2012) Intelligent fuzzy- PID temperature controller design of drying system. In: 2012 International conference on information management, innovation management and industrial engineering (ICIII), 20–21 Oct 2012, pp 54–57

Minglin Y (2010) Realization of Fuzzy PID controller used in turbine speed control system with FPGA. 2010 international conference on future information technology and management engineering (FITME), 9–10 Oct 2010, pp 261–264

Mustafa M, Al Gizi AJ (2013) Hybrid neural-genetic and fuzzy logic approach for real-time tuning of PID controller to improve the system frequency response of AVR system. Life Sci J 10(4):2714–2724

Pan I, Das S (2012a) Chaotic multi-objective optimization based design of fractional order PIλDμ controller in AVR system. Int J Electr Power Energy Syst 43(1):393–407

Pan I, Das S (2012b) Intelligent fractional order systems and control: an introduction. Springer, New York

Pan I, Das S (2013) Frequency domain design of fractional order PID controller for AVR system using chaotic multi-objective optimization. Int J Electr Power Energy Syst 51:106–118. https://doi.org/10.1016/j.ijepes.2013.02.021

Pan I, Das S (2015) Fractional-order load-frequency control of interconnected power systems using chaotic multi-objective optimization. Appl Soft Comput 29:328–344

Panda S, Sahu BK, Mohanty PK (2012) Design and performance analysis of PID controller for an automatic voltage regulator system using simplified particle swarm optimization. J Frankl Inst 349(8):2609–2625. https://doi.org/10.1016/j.jfranklin.2012.06.008

Prasad LB, Gupta HO, Tyagi B (2014) Application of policy iteration technique based adaptive optimal control design for automatic voltage regulator of power system. Int J Electr Power Energy Syst 63:940–949

Qasem SN, Shamsuddin SM (2011) Memetic elitist pareto differential evolution algorithm based radial basis function networks for classification problems. Appl Soft Comput 11(1):5565–5581

Rahimian MS, Raahemifar K (2011) Optimal PID controller design for AVR system using particle swarm optimization algorithm. In: 2011 24th Canadian conference on electrical and computer engineering (CCECE), 8–11 May 2011, pp 000337–000340

Rajasekhar A, Jatoth RK, Abraham A (2014) Design of intelligent PID/PI λ. D μ speed controller for chopper fed DC motor drive using opposition based artificial bee colony algorithm. Eng Appl Artif Intell 29:13–32

Ramezanian H, Balochian S, Zare A (2013) Design of optimal fractional-order PID controllers using particle swarm optimization algorithm for automatic voltage regulator (AVR) system. J Control Autom Electr Syst 5(24):601–611

Sahib MA (2015) A novel optimal PID plus second order derivative controller for AVR system. Eng Sci Technol Int J 18(2):194–206

Shamisa A, Karrari M, Malik OP (2008) Power system transient stability assessment using on-line measurement data. Int Rev Electr Eng 3(4):653–661

Shivakumar R, Lakshmipathi R, Panneerselvam M (2010) Power system stability enhancement using bio inspired genetic and PSO algorithm implementation. Int Rev Electr Eng 5(4):1609–1615

Simoes MG, Bose BK, Spiegel RJ (1997) Fuzzy logic based intelligent control of a variable speed cage machine wind generation system. IEEE Trans Power Electron 12(1):87–95

Sinthipsomboon K, Hunsacharoonroj I, Khedari J, Pongaen W, Pratumsuwan P (2011) A hybrid of fuzzy and fuzzy self-tuning PID controller for servo electro-hydraulic system. In: 2011 6th IEEE

conference on industrial electronics and applications (ICIEA), 21–23 June 2011, pp 220–225

Soundarrajan A, Sumathi S (2010) Fuzzy-based intelligent controller for power generating systems. J Vib Control. https://doi.org/10.1177/1077546310371347

Su H, Hao G, Li P, Luo X (2010) Feed forward fuzzy PID controller for common-rail pressure control of diesel engine. In: 2010 international conference on measuring technology and mechatronics automation (ICMTMA), 13–14 March 2010, pp 264–267

Tang Y, Cui M, Hua C, Li L, Yang Y (2012) Optimum design of fractional order PIλDμ controller for AVR system using chaotic ant swarm. Expert Syst Appl 39(8):6887–6896

Vural AM, Bayindir KC (2012) Transient stability enhancement of the power system interconnected with wind farm using generalized unified power flow controller with simplex optimized self-tuning fuzzy damping scheme. Int Rev Electr Eng 7(4):5091–5107

Wahab NIA, Mohamed A (2010) Transient stability emergency control using generator tripping based on tracking area-based rotor angle combined with UFLS. Int Rev Electr Eng 5(5):2317–2326

Wong C-C, An LS, Wang H-Y (2009) Optimal PID controller design for AVR system. Tamkang J Sci Eng 12(3):259–270

Yao-Lun L, Chia-Chang T, Wu-Shun J, Shuen-Jeng L (2007) Design an intelligent neural-fuzzy controller for hybrid motorcycle. In: Fuzzy information processing society, 2007. NAFIPS '07. Annual meeting of the North American, 24–27 June 2007, pp 283–288

Yeroğlu C, Ateş A (2014) A stochastic multi-parameters divergence method for online auto-tuning of fractional order PID controllers. J Frankl Inst 351(5):2411–2429

Yu GR, Hwang RC (2004) Optimal PID speed control of brushless DC motors using LQR approach. In: IEEE international conference system, man, and cybernetics, pp 473–478

Zeng G-Q, Chen J, Dai Y-X, Li L-M, Zheng C-W, Chen M-R (2015) Design of fractional order PID controller for automatic regulator voltage system based on multi-objective extremal optimization. Neurocomputing 160:173–184

Zhang Xiao M, Long Shi Y (2012) Simulation study on fuzzy PID controller for DC motor based on DSP. In: 2012 international conference on industrial control and electronics engineering (ICICEE), 23–25 Aug 2012, pp 1628–1631